The Effect of SiO2 Content and Shape on Mechanical Properties of Al Matrix Composites

Davoud Khademi
Ferdowsi University of Mashhad
Elahe Khodeir (elahe.khodeir@gmail.com)
Ferdowsi University of Mashhad Faculty of Engineering
Seyed Mostafa Mahdizadeh
Ferdowsi University of Mashhad
Hamideh Yari
Ferdowsi University of Mashhad

Original Research

Keywords: Aluminum composite, nanoparticle, nanotube, SiO2, mechanical properties

Posted Date: February 1st, 2021

DOI: https://doi.org/10.21203/rs.3.rs-162183/v1

The effect of SiO_2 content and shape on mechanical properties of Al matrix composites

Davoud Khademi[1,3], Elahe Khodeir[2, 3,*], Seyed Mostafa Mahdizadeh[2], Hamideh Yari[2]

1 Department of Materials Science and Engineering, Faculty of Engineering Ferdowsi University of Mashhad, Iran
2 Department of Chemical Engineering, Faculty of Engineering, Ferdowsi University of Mashhad, Mashhad, Iran
3 Central laboratory of Ferdowsi University of Mashhad, Iran

[*] *Corresponding author. Tel: +989150467914*
Email address: Elahe.khodeir@gmail.com

Abstract

Physical properties and processing parameters of the reinforcing phase such as shape and content can dramatically influence the mechanical properties of the composites. In this project, the effect of different shapes of silicon dioxide or silica (SiO_2) reinforcement including nanoparticle and nanotube as well as their weight percent (1, 3, 5 and 10 wt %) on the mechanical properties of aluminum (Al) composite were investigated. The silica nanotubes (SNTs) were prepared by hydrothermal methods. In order to achieve a good dispersion, Al powders were coated by cetyl trimethyl ammonium bromide (CTAB) to obtain a surface positive charge. Then, SiO_2–Al powders were obtained by electrostatic self-assembly to realize the homogeneous adsorption of SiO_2 nano reinforcement on Al powders. Finally, SiO_2-reinforced Al matrix composites were fabricated by powder metallurgy.

Characterization of composites was carried out by transmission electron microscopy (TEM), field emission scanning electron microscopy (FESEM) and Fourier transform infrared spectroscopy (FTIR). For determination of the mechanical properties of the composite, the compressive strength and density were investigated.

Results showed a significant reduction in the relative density from 98% to 84% for composites containing 0 to 10 wt % of SiO_2. The compressive strength exhibited a moderate increase by adding SNTs while in samples containing SiO_2 nanoparticles, the mechanical properties improved and reached a peak value of 225 MPa at 5 wt % SiO_2 nanoparticles (~40% increase compared to pure Al). However, a further increase in nanotubes content resulted in a considerable reduction in compressive strength. This can be attributed to the increase in porosity and agglomeration of nano reinforcement in the composite.

Key words: Aluminum composite, nanoparticle, nanotube, SiO_2, mechanical properties.

1. Introduction

Aluminum matrix nanocomposites (AMNCs) are an important type of composite for many industrial products such as automotive body and airframe due to their low density and high strength to weight ratio [1]. The most important composite manufacturing processes for fabrication of aluminum (Al) matrix composite is powder metallurgy, which involves the application of pressure and heat in a controlled atmosphere [2]. During composite preparation, adding small amounts of different reinforcements to the Al matrix leads to a significant improvement in mechanical properties of the composite. In previous studies, different shapes of the reinforcing phase (such as particulates, whiskers or fiber) and various nanoparticles (including Al_2O_3 [3], MgO [4], ZrO_2 [5], SiC [6] and SiO_2 [7]) were used to synthesize Al matrix nanocomposites.

Among these nanoparticles, amorphous ceramic nanoparticles seem to be an appropriate material for reinforcing metal matrix composites (MMCs), due to their unique mechanical and physical properties. Silica has several applications in electronic parts of printer toners and the pharmaceutical industry. Al matrix composites with silica reinforcement usually exhibit superior mechanical properties compared to monolithic materials, particularly in severe working conditions such as elevated temperatures [1, 8, 9]. On the other hand, among one-dimensional nanostructured materials, silica nanotubes (SNTs) have been extensively used in catalysis, biosensor, nanoscale electronics, storage and delivery systems due to important features of accessibility, biocompatibility and photoluminescence [10]. Various methods were introduced by researchers for synthesis of SNTs. Yin et al. [11] applied multi-walled carbon nanotube (MWCNT) as a template to synthesize SNTs. Zhang et al. [12] synthesized SNTs with orientation-controlled mesopores by interfacial growth using porous anodic alumina (PAA) and polycarbonate membranes as a rigid template. Kaifeng et al. [13] prepared and characterized single-crystal SNTs. Ananth et al. [14] introduced a novel method of SNT preparation on an anodic alumina membrane in the presence of phosphoric acid.

In the present work, mesostructured SNTs have been synthesized in a system of carbon nanotubes (CNTs)/cetyl trimethylammonium bromide (CTAB)/tetraethylorthosilicate (TEOS)/$NH_3.H_2O$ through one-pot hydrothermal route [10]. This method leads to a facile technique for the synthesis of porous hollow SNTs [15]. The aim of the present study is to show how the physical property and processing parameters influence the mechanical properties of Al-based metal matrix

composites reinforced by nanoparticles and SNTs with 1, 3, 5 and 10 wt % SiO_2 which is synthesized by powder metallurgy sintering.

2. Experimental

2.1 Synthesis of SNTs

The raw materials used for the SNT synthesis included CTAB (MW: 364.45 g/mol), $NH_3.H_2O$ (25%) solution, and CNTs as a template [10]. TEOS (99%) was obtained from Merck. CNTs with an outside diameter of ≤50 nm and inside diameter of ≤30 nm were applied as a soft template.
Fig. 1 illustrates the image of the CNTs characterized using transmission electron microscopy (TEM).

Fig. 1. TEM images of CNTs

SNTs were synthesized via a method reported by Wang et al. [10]. Initially 2.4 g of CTAB with 14 mL of $NH_3.H_2O$ was stirred for 15 min. Then, 1.2 g of CNTs was gradually added into the solution and stirred for 3 h at room temperature. Next, TEOS (99%) was added and the solution was further stirred for 2 h. The homogenous solution was placed into an autoclave at a temperature of 100 °C for 72 h. Finally, the sample was centrifuged and washed, dried at 50 °C and calcined at 700 °C in final step to remove the template [15]. The schematic of synthesis of SNTs is illustrated in Fig. 2.

Fig. 2. The schematic of synthesis of SNTs

2.2 Fabrication of the Al–SiO_2 powders

In order to produce the composites, the following starting powders were used: Al with an average particle size of 45 μm and 99% purity as the matrix, SiO_2 nanoparticles with an average particle size about 60 nm, and SNTs (produced in the previous step) with an outside diameter of ≤100 nm as the reinforcing phase. Fig. 3 shows TEM and field emission scanning electron microscopy (FESEM) images of the raw materials and their energy-dispersive X-ray spectroscopy (EDS) analysis.

Fig. 3. TEM and FESEM images of raw materials. a) SNTs, b) SiO_2 nanoparticle, c) Al powder

1 g of the cation surfactant CTAB was added into distilled water and dispersed by stirring at 50 °C to obtain 1 wt % CTAB aqueous solution. Then, 10 g of pure Al powders were added to the solution and sonicated for 20 min, followed by stirring for 1 h at room temperature. The powders were filtered and washed with distilled water to remove unreacted CTAB and obtain the CTAB coated Al powders. Then, the powders were added into distilled water to form a suspension under stirring. Meanwhile, SiO_2 powder with a certain ratio to achieve composites (1, 3, 5 and 10 wt %) were put into 50 mL of distilled water and ultrasonically treated for 1 h for appropriate dispersion. Finally, the Al powders suspension and SiO_2 dispersion were mixed, stirred and filtered to obtain the Al-SiO_2 powders.

The mixed powders were placed in a cylindrical stainless-steel die (with 10 mm diameter and 15 mm length) and compacted using a hydraulic press at a pressure of 800 MPa with tolerances of 0.1 mm along the length. The compacts were then sintered in a horizontal tube furnace at 625 °C in argon atmosphere. The schematic of fabrication process of the Al-SiO_2 composite is shown in Fig. 4.

Fig. 4. The schematic of fabrication process of the Al-SiO_2 composite

In order to investigate the effect of nanoparticles and nanotubes of SiO_2 on the mechanical properties of the composite, uniaxial compressive and relative density tests were carried out. In the samples prepared by powder metallurgy, it is very important to achieve a high density close to the theoretical density [16, 17]. In this study, compressive strength tests were performed on cylindrical specimens using a Zwick model Z250 universal test machine at room temperature with a strain rate of 0.103 s^{-1}. According to the ASTM E9, the height to diameter ratio was 1.5 and the test continued until the sudden drop in stress occurred that was considered as the failure phase.

The theoretical composite density after polishing was calculated by ASTM B962-14. Based on this method, the weight of sample in air and distilled water was measured. The theoretical Al matrix nanocomposite density (ρ_{AMNC}) was calculated using Eq. (1):

$$\rho_{AMNC} = \frac{A}{A-B}\rho_0 \quad (1)$$

where A is the mass of the composite in air, B is the mass of the same composite in distilled water, and ρ_0 is the density of the distilled water. The absolute porosity (p) of the sample was calculated according to Eq. (2):

$$p = \frac{\rho_{th} - \rho_{AMNC}}{\rho_{th}} \quad (2)$$

where ρ_{th} and ρ_{AMNC} are theoretical and effective densities, respectively [18]. Theoretical density ρ_{th} was calculated for each powder mixture based on the rule of mixtures approach:

$$\rho_{th} = \rho_m v_m + \rho_{r.f} v_{r.f} \quad (3)$$

where $\rho_m$and $\rho_{r.f}$ are densities of the matrix and reinforcement, respectively. Also, v_m and $v_{r.f}$ are volume fractions of matrix and reinforcement, respectively [17].

3. Results and discussion

3.1 Chemical components of SNTs

Fig. 5 illustrates the Fourier transform infrared (FTIR) spectrum of SNT before and after calcination at 750 °C. Before calcination, the characteristic bands are exhibited in spectra for Si–O–Si (1078, 792 and 461cm^{-1}), Si-OH (963 and 1634 cm^{-1}) and C–H (2921, 2851,718 and 1466 cm^{-1}) while, after calcination, only bands related to O-Si-O bending vibration were observed and other bands disappeared. In addition, the intensities of the bands for O-Si-O were increased which confirmed that the template was passivated by calcination.

Fig. 5. FTIR spectra of SiO_2 nanotube before and after calcination

3.2 Distribution of SiO_2 in Al matrix

In order to measure zeta potential of nanoparticles of SiO_2, Al, CTAB and Al-CTAB, 10 mg of each material was suspended in 150 mL of deionized water and pH of each solution was found to be 6.5. It can be seen in Table 1 that zeta potential of Al and nanoparticles of SiO_2 was around -25 mV. This negative charge prevents the particles from attracting each other. With the addition of CTAB, negative charged Al dissociated by CTAB was adsorbed on the surface of particles to

neutralize the original negative charges, resulting in a change in surface charge of the Al powder from negative to positive [19]. As a result, the electrostatic repulsion between Al and Si was decreased and the dispersion behavior was significantly improved. Therefore, silica species could be coated on the surface of Al.

Table 1. Zeta potential of SiO_2, Al, CTAB and Al-CTAB under PH=6.5

Controlling the distribution of reinforcement between Al powders is known to be the main issue for creating high performance composites. This issue is directly related to the mechanical properties of the composite [20]. Fig. 6 shows FESEM images and EDS analysis of composites containing SiO_2 nanoparticles (3, 5 and 10 wt %). As can be observed, the uniform distribution of nanoparticles on the Al surface is clear in the sample containing 3 wt % SiO_2. However, agglomeration of nanoparticles is observed with the increase in the weight percentage of SiO_2 in composites. In addition, in the EDS spectra of the composites, a weak peak of C appeared. This may be related to the presence of CTAB in the composite.

Fig. 6. Distribution of a) 3 wt %, b) 5 wt % and c) 10 wt % SiO_2 nanoparticles on Al powders

Distribution of SNTs within the Al powder is shown in Fig. 7. According to previous results, a uniform distribution can be seen in the samples containing 3 and 5 wt % SNTs. Furthermore, agglomeration of the SNTs was observed in the samples containing 10 wt % SNT. Bonding between the particles within agglomerates is weak and the rearrangement that occurred resulted in the formation of large pores.

Fig. 7. Distribution of a) 3, b) 5 and c) 10 wt % SNTs on Al powders

Fig. 8 shows the polished surface of composites after sintering at 625 ^{o}C for 1.5 h. It can be observed that effective sintering of pure Al resulted in particles that were well connected together

with no porosity. Moreover, in the samples containing 3 and 5 wt % SiO_2, the powder particles connected well together and a uniform distribution of Al particles can be seen.

Fig. 8. FESEM images of polished surface of composites a) pure Al, b) 3 wt % and c) 5 wt % SiO_2 nanoparticles

In addition, agglomerated bulk reinforcements were observed in the samples containing 10 wt % SNTs and nanoparticles (Fig. 9). During polishing, these agglomerates, which formed with increase in weight percent of SiO_2, can be detached from the surface of composite [21].

Fig. 9. The FESEM images of the composite containing 10 wt % a) SNTs, b) SiO_2 nanoparticles after sintering

3.3 The effect of SiO_2 on relative density of the composite

Since the density of Al (2.7 g/cm^3) and SiO_2 (2.64 g/cm3) are close to each other, it is expected that the density of Al-SiO_2 composite does not change significantly with the addition of SiO_2. According to Fig. 10, however, the relative density of the composite decreased with the addition of the reinforcement particles. This behavior can be attributed to the presence of rigid SiO_2 particles, which reduced the compressibility of the composite, increasing the porosity and consequently decreasing the density [3].

On the other hand, by enhancing the weight percentage of reinforcing particles, the number of pores and defects within the sample could be increased. It can be seen that in the samples containing 1 wt % SiO_2, the difference between the densities of reinforcement particle for nanoparticles was not obvious compared to SNTs.

In contrast, an increase in SiO_2 content resulted in a decrease in density of Al-SNT composite. Potentially the presence of the nanotubes reduces the compressibility of the sample. On the other hand, the empty inner space of SNTs may decrease the density [3]. Additionally, by increasing the SNT content to 10 wt %, the difference between the densities of composites with SNTs and nanoparticles was reduced. Increase in the nanoparticle content in comparison with SNTs might decrease the compressibility of the powder, increasing the porosities in these samples.

Fig. 10. Relative density of the composite as a function of SiO_2 weight percent

3.4 The effect of SiO_2 on compressive strength of the composite

Fig. 11. Compressive strength of the composite as a function of SiO_2 weight percent

Fig. 11 depicts the effect of SiO_2 weight percent on the compressive strength of the composite. It can be observed that in all samples containing both SiO_2 nanoparticles (1, 3 and 5 wt %) and SNTs, the compressive strength was higher than in pure Al. In these samples, sliding and debonding between Al matrix and SNTs were probably prevented by SiO_2, leading to an increase in compressive strength. Also, this rigid reinforcement behaved as an obstacle to crack growth and, as a result, contributing to enhancement of the compressive strength of the composite [22].

Furthermore, in the composites containing SNTs, three strengthening mechanisms could increase the compressive strength of the composite, in addition to the presence of rigid particle of silica. These mechanisms include load transfer, generation of dislocations by thermal mismatch, and the Orowan looping system that are summarized in Eq. (4) [20]:

$$\boldsymbol{\sigma_C = \sigma_M + \Delta\, \sigma_{L.T} + \Delta\, \sigma_{T.M} + \Delta\, \sigma_{Orowan}} \quad (4)$$

Where σ_C is the strength of the composite, σ_M is the strength of the matrix, $\Delta\, \sigma_{L.T}$ is the improved strength related to load transfer, $\Delta\, \sigma_{T.M}$ is the improved strength associated with the generation of dislocations by thermal mismatch and $\Delta\, \sigma_{Orowan}$ is the improved strength due to the Orowan looping system [20].

The shear lag model suggested by Kelly and Tyson for fiber-reinforced composites which is the basis of load transfer theory, can be used to analyze the strengthening of composites containing nanotube reinforcements. The stress applied through interfacial shear stress is transferred from the matrix to the fibers [14].

The coefficients of thermal expansion of SiO_2 and Al are 5.5×10^{-7} $°C^{-1}$ and 2.5×10^{-5} $°C^{-1}$, respectively. Therefore, the significant difference between thermal expansion coefficients of these two materials causes large thermal stresses around reinforcements. Consequently, plastic deformation in the matrix and dislocation loops around the nano-reinforcements lead to a strengthened nanocomposite.

According to the Orowan mechanism, the strength of the composite material may be increased by improvement in the interaction between reinforcements and the dislocation [18].

As can be seen, in the composites prepared through adding the nanoparticle-reinforcement, the compressive strength was higher than in SNT-reinforced samples. In fact, with the change in the

shape of reinforcement, the empty spaces of the nanotube-composites were filled in the nanoparticle-composite and the distance between nanoparticles decreased with the increase in filler content. Hence, this led to a higher compressive strength, based on the Orowan theory. Moreover, according to the theory of mismatch of thermal expansion coefficient, the number of sites for crack initiation was increased. All the theoretical calculations based on the above mechanism were performed. However, they were different from the experimental results due to ignoring interfacial defects.

In addition, the compressive strength was decreased in the samples containing 10 wt % SiO_2. It would appear that their agglomeration in the composite increased with the increase in the weight percent of reinforcements. Also, difficult compression of the rigid SiO_2 particles leads to a reduction in density and increase in porosity of the composites. Particle distribution in Al matrix is affected by porosity and agglomeration. Thus, compressive strength of the sample containing 10 wt % SiO_2 was decreased [3].

3.5 The effect of SiO_2 on failure strain of the composite

It can be seen in Fig. 12 that the final strain of the composite was decreased with the increase in the amount of reinforcement. This might be due to reduction of the distance between the rigid particles of reinforcements by increasing their number, resulting in a reduced deformation of the composite. Therefore, the growth of cracks occurred at a lower strain in the composites containing SiO_2 compared to those with pure Al. On the other hand, the amount of reinforcement and the obstacles for dislocation motion increased with the decrease in particle size [23]. Considering the above reasons, the strain for samples modified with nanoparticles is less than for SNTs.

Fig. 12. Final strain of composite as a function of SiO_2 weight percent

Fig. 13 shows FESEM images of fracture surfaces of the samples containing 5 wt % SNTs and nanoparticles. As can be observed, in addition to homogenous dispersion of SNTs throughout the composites, strengthening mechanisms including fracture and pull-out of SNTs can be found clearly [24]. Additionally, in the case of SiO_2 nanoparticles, their uniform distribution and strong bond with the Al matrix can be seen as well. Therefore, the strength of the composite is improved by adding the effective amount of reinforcement.

Fig. 13. Fracture surface of the composite containing 5 wt % a) SNTs, b) SiO_2 nanoparticles

The fracture surface of the sample containing 10 wt % SiO_2 nanoparticles is illustrated in Fig. 14. According to this figure, the agglomerated reinforcement particles on the surface of the sample can be observed. Moreover, the agglomerates can provide desired sites for nucleation and growth of cracks [25]. On the other hand, by increasing the weight percent of SiO_2, particles covered the surface of Al and performed as obstacles during sintering. So, the weak bonding between Al particles can be destroyed during compressive strength analysis.

Fig 14. Fracture surface of the composite containing 10% SiO_2 nanoparticles

4. Conclusions

The Al-based metal matrix composites with SiO_2 nanoparticles and nanotubes reinforcement were prepared via powder metallurgy method using CTAB as a binding agent. Also, the effect of weight percent of silica on mechanical properties of the composite was studied. The results showed that the parameters such as the relative density and ultimate failure strain of the composite were decreased with the increase in the SiO_2 content to 5% in both types of filler. This was attributed to rigid particles of SiO_2 which causes reduction of the flexibility and compressibility in the composite. On the other hand, in the composites containing nanoparticles and SNTs, the compressive strength was greater than in pure Al. This might be due to the movement of dislocations generated between the matrix and the reinforcement particles prevented by SiO_2, causing increase in the compressive strength. Accordingly, the highest compressive strength is attributed to the sample containing 5 wt % SiO_2 nanoparticles. Based on strengthening mechanisms, the distance between nanoparticles might decrease, thus λ was decreased which led to an increase in the compressive strength. In addition, the number of sites for crack initiation increased.

Acknowledgement

The authors wish to express their appreciation to staff of central laboratory of Ferdowsi University of Mashhad for their kind support and contribution to the paper.

Conflict of Interest

The authors declare that they have no conflict of interest.

Funding statement

The authors declare that they have no known competing financial interests or personal relationships that could have appeared to influence the work reported in this paper.

Author contributions

Davoud.Khademi, Elahe.Khodeir, Seyed Mostafa.Mahdizadeh and Hamideh.Yari contributed to the design and implementation of the research, to the analysis of the results and to the writing of the manuscript.

Availability of data and material

The authors confirm that the data supporting the findings of this study are available within the article and its supplementary materials.

Compliance with ethical standards

Not applicable

Consent to participate

Not applicable

Consent for publication

Not applicable

Reference

1. Issa, H.K., et al., *Development of an aluminum/amorphous nano-SiO2 composite using powder metallurgy and hot extrusion processes.* Ceramics International, 2017. **43**(17): p. 14582-14592.
2. Maleki, A., B. Niroumand, and M. Meratian, *Effects of processing temperature on in-situ reinforcement formation in Al (Zn)/Al2O3 (ZnO) nanocomposite.* Metallurgical and Materials Engineering, 2015. **21**(4): p. 283-291.

3. Beheshtipour, A., et al., *Comparison of Mechanical Properties and Corrosion Behavior of Al-NanoAl 2 O 3 with Al-MicroAl 2 O 3 Composites Made by SPS Process.* Metals and Materials International, 2019: p. 1-13.
4. Abdizadeh, H., R. Ebrahimifard, and M.A. Baghchesara, *Investigation of microstructure and mechanical properties of nano MgO reinforced Al composites manufactured by stir casting and powder metallurgy methods: A comparative study.* Composites Part B: Engineering, 2014. **56**: p. 217-221.
5. Ramachandra, M., et al., *Hardness and wear resistance of ZrO2 nano particle reinforced Al nanocomposites produced by powder metallurgy.* Procedia Materials Science, 2015. **10**: p. 212-219.
6. El-Kady, O. and A. Fathy, *Effect of SiC particle size on the physical and mechanical properties of extruded Al matrix nanocomposites.* Materials & Design (1980-2015), 2014. **54**: p. 348-353.
7. Zhu, H., et al., *Reaction mechanism and mechanical properties of an aluminum-based composite fabricated in-situ from Al–SiO2 system.* Materials Chemistry and Physics, 2014. **145**(3): p. 334-341.
8. Cavaliere, P., et al., *Influence of SiO2 nanoparticles on the microstructure and mechanical properties of Al matrix nanocomposites fabricated by spark plasma sintering.* Composites Part B: Engineering, 2018. **146**: p. 60-68.
9. Wang, K., et al., *Thermal analysis of in-situ Al2O3/SiO2 (p)/Al composites fabricated by stir casting process.* Thermochimica Acta, 2016. **641**: p. 29-38.
10. Wang, L., et al., *One-pot hydrothermal synthesis of mesostructured silica nanotube.* Journal of colloid and interface science, 2009. **335**(2): p. 264-267.
11. Yin, Z.-H., X. Liu, and Z.-X. Su, *Novel fabrication of silica nanotubes using multi-walled carbon nanotubes as template.* Bulletin of Materials Science, 2010. **33**(4): p. 351-355.
12. Zhang, A., et al., *Synthesis of silica nanotubes with orientation controlled mesopores in porous membranes via interfacial growth.* Chemistry of Materials, 2012. **24**(6): p. 1005-1010.
13. Yu, K., et al., *Preparation and Characterization of Single-Crystal Silica Nanotubes.* Synthesis and Reactivity in Inorganic, Metal-Organic, and Nano-Metal Chemistry, 2015. **45**(5): p. 770-772.
14. Prem Ananth, K., et al. *A Novel Modified sol-gel template Synthesis of high aspect ratio silica nanotubes in the presence of Phosphoric Acid*. in *Journal of Nano Research*. 2016. Trans Tech Publ.
15. Yari, H., M. Pakizeh, and M. Namvar-Mahboub, *Effect of silica nanotubes on characteristic and performance of PVDF nanocomposite membrane for nitrate removal application.* Journal of Nanoparticle Research, 2019. **21**(5): p. 94.
16. Bram, M., et al., *Powder metallurgical fabrication processes for NiTi shape memory alloy parts.* Materials Science and Engineering: A, 2002. **337**(1-2): p. 254-263.
17. Nassar, A.E. and E.E. Nassar, *Properties of aluminum matrix Nano composites prepared by powder metallurgy processing.* Journal of king saud university-Engineering sciences, 2017. **29**(3): p. 295-299.
18. Sadeghi, B., et al., *Effect of processing parameters on microstructural and mechanical properties of aluminum–SiO2 nanocomposites produced by spark plasma sintering.* International Journal of Materials Research, 2018. **109**(5): p. 422-430.
19. Khan, A.M., et al., *Surface modification of colloidal silica particles using cationic surfactant and the resulting adsorption of dyes.* Journal of Molecular Liquids, 2019. **274**: p. 673-680.
20. Park, J.G., D.H. Keum, and Y.H. Lee, *Strengthening mechanisms in carbon nanotube-reinforced aluminum composites.* Carbon, 2015. **95**: p. 690-698.
21. Nadar, A., et al., *Nanostructured Fe2O3 dispersed on SiO2 as catalyst for high temperature sulfuric acid decomposition—Structural and morphological modifications on catalytic use and relevance of Fe2O3-SiO2 interactions.* Applied Catalysis B: Environmental, 2017. **217**: p. 154-168.
22. Urata, S., et al., *Adhesion between copper and amorphous silica: A reactive molecular dynamics study.* The Journal of Physical Chemistry C, 2018. **122**(49): p. 28204-28214.

23. Aktaş, S. and E.A. Diler, *A review on the effects of micro-nano particle size and volume fraction on microstructure and mechanical properties of metal matrix composites manufactured via mechanical alloying.* International Advanced Researches and Engineering Journal, 2018. **2**(1): p. 68-74.
24. Wang, Y., X. Qiu, and J. Zheng, *Study the mechanism that carbon nanotubes improve thermal stability of polymer composites: An ingenious design idea with coating silica on CNTs and valuable in engineering applications.* Composites Science and Technology, 2018. **167**: p. 529-538.
25. Boccaccini, D.N., et al., *Influence of porosity on mechanical properties of tetragonal stabilized zirconia.* Journal of the European Ceramic Society, 2018. **38**(4): p. 1720-1735.

Figures

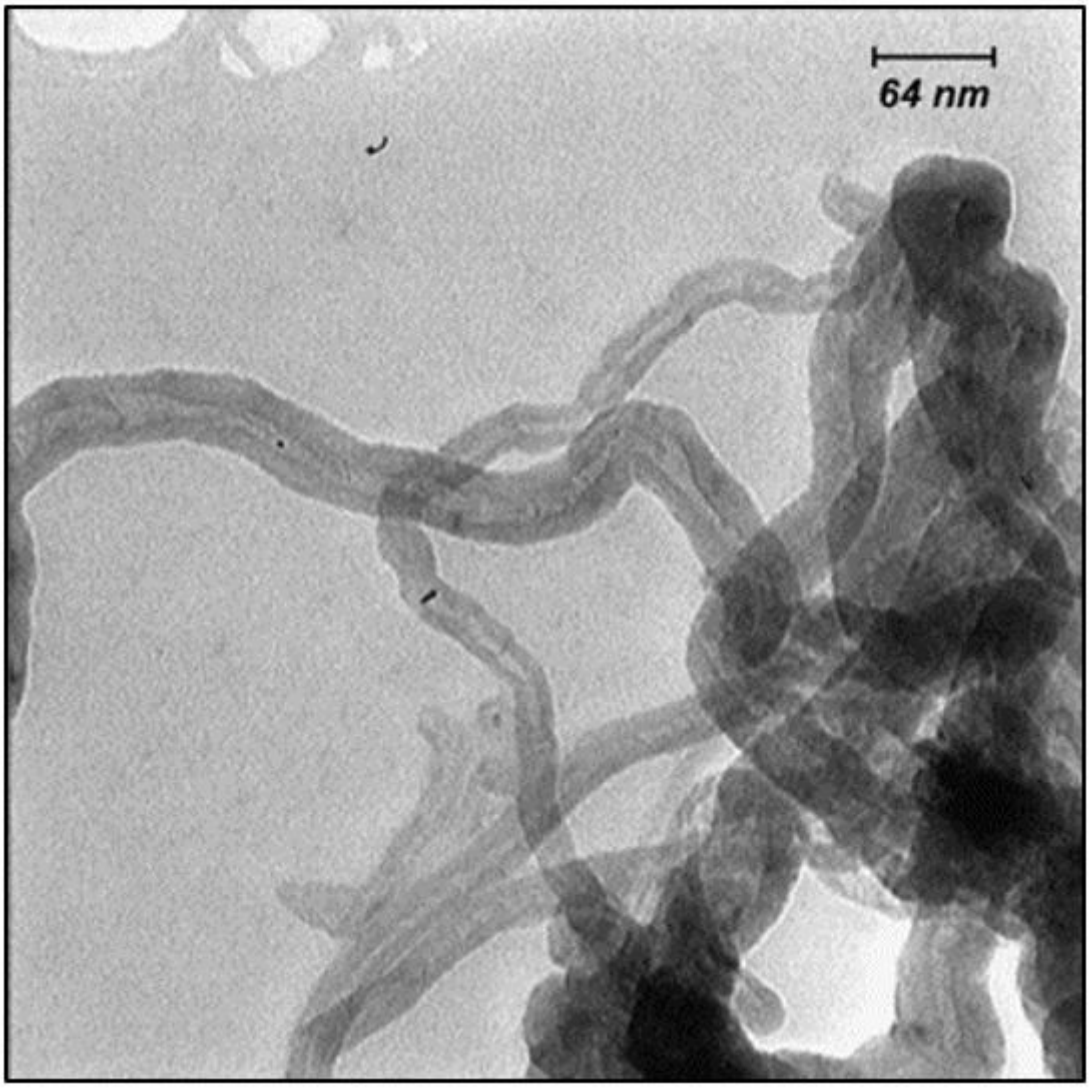

Figure 1

TEM images of CNTs

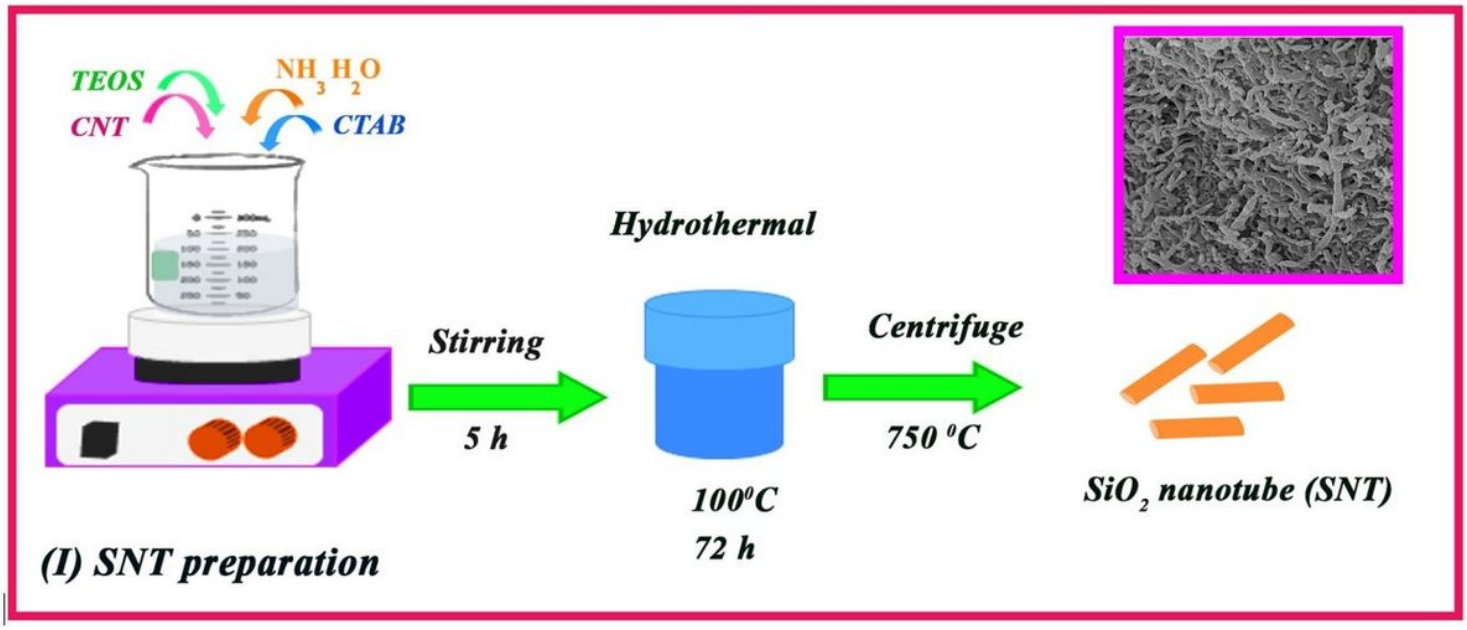

Figure 2

The schematic of synthesis of SNTs

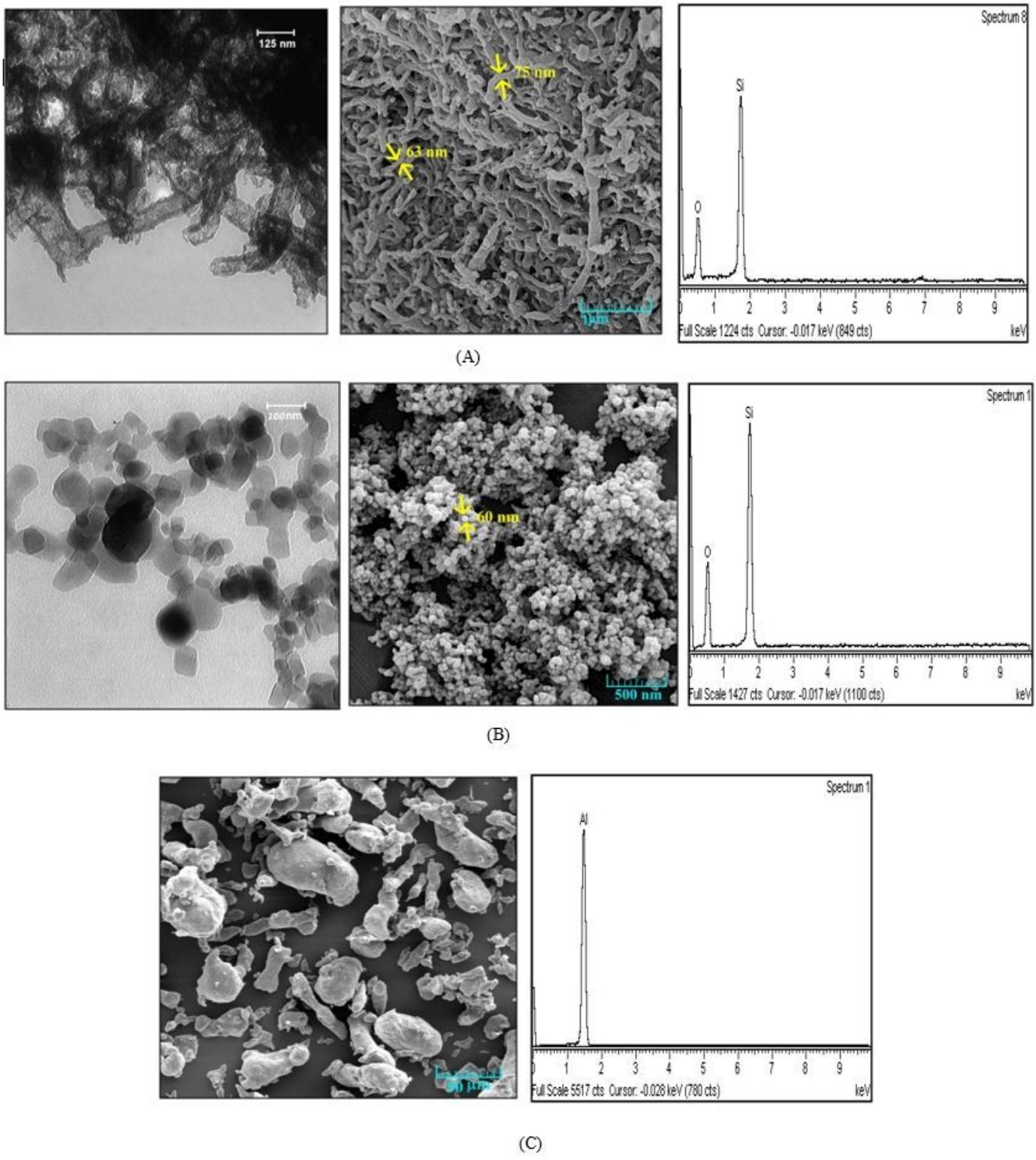

Figure 3

TEM and FESEM images of raw materials. a) SNTs, b) SiO2 nanoparticle, c) Al powder

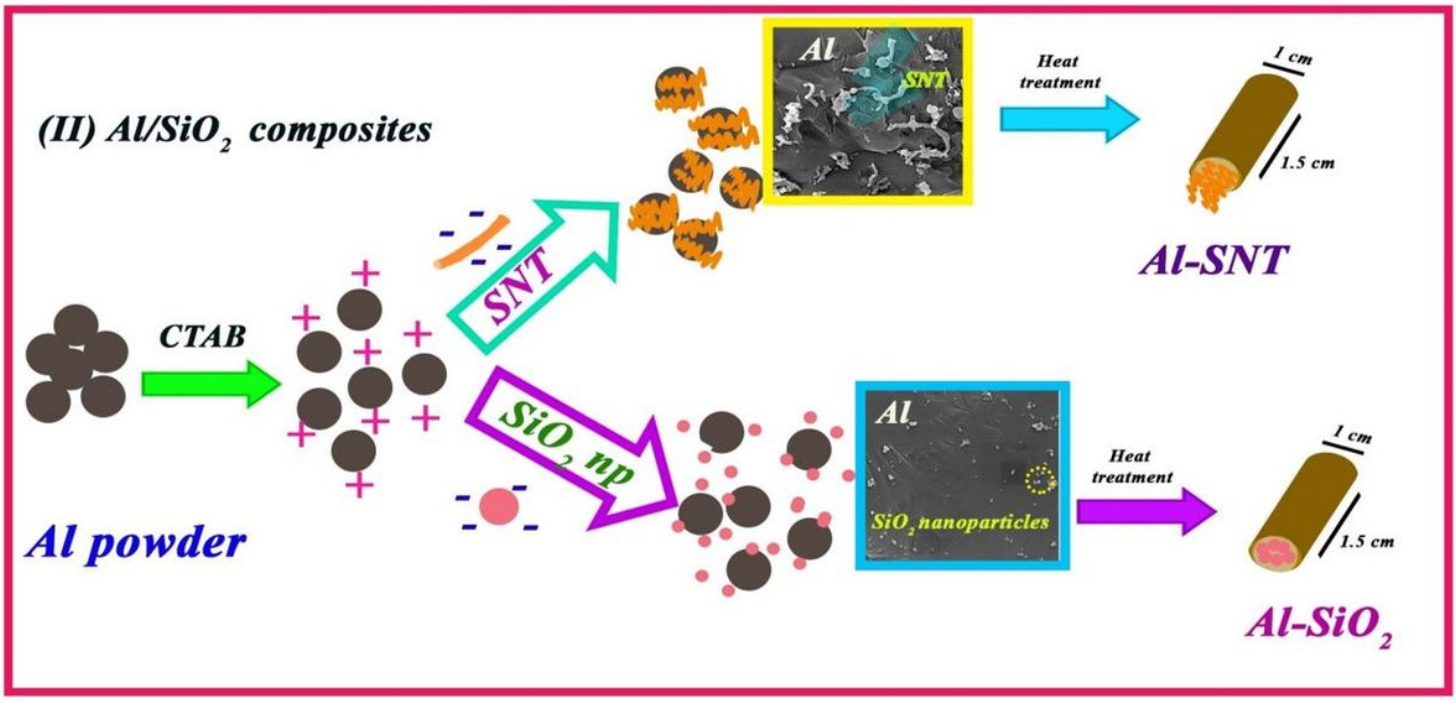

Figure 4

The schematic of fabrication process of the Al-SiO2 composite

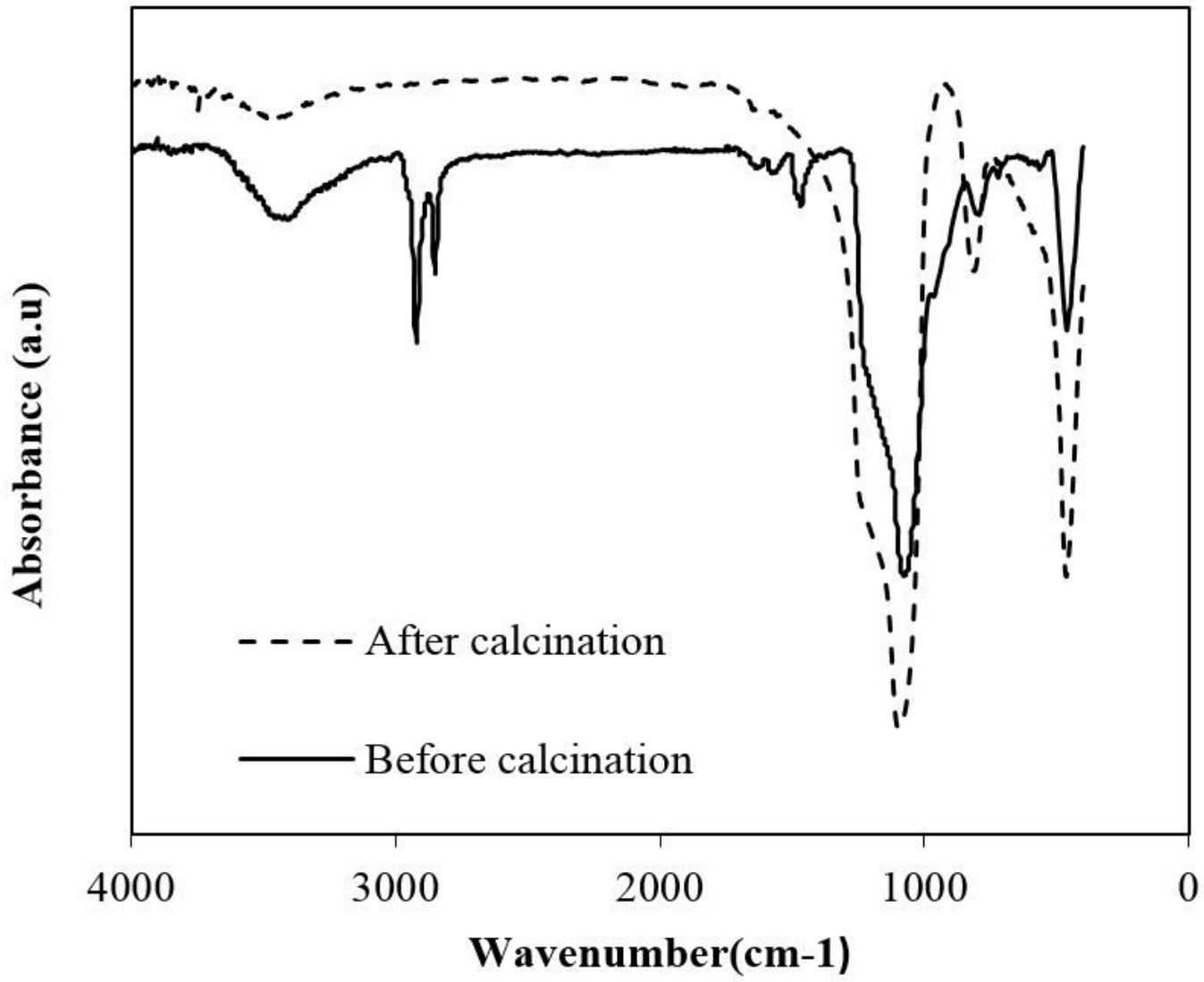

Figure 5

FTIR spectra of SiO2 nanotube before and after calcination

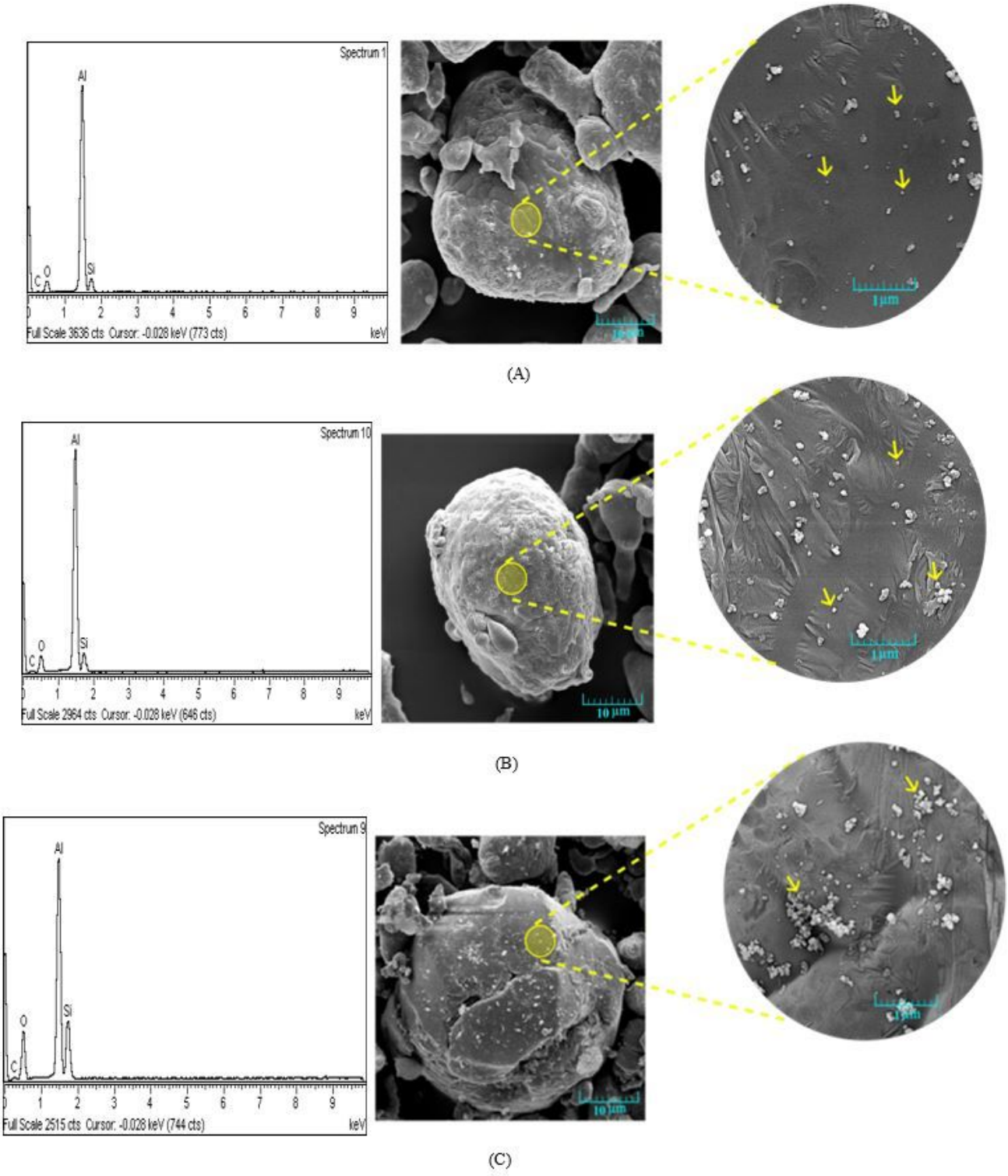

Figure 6

Distribution of a) 3 wt %, b) 5 wt % and c) 10 wt % SiO2 nanoparticles on Al powders

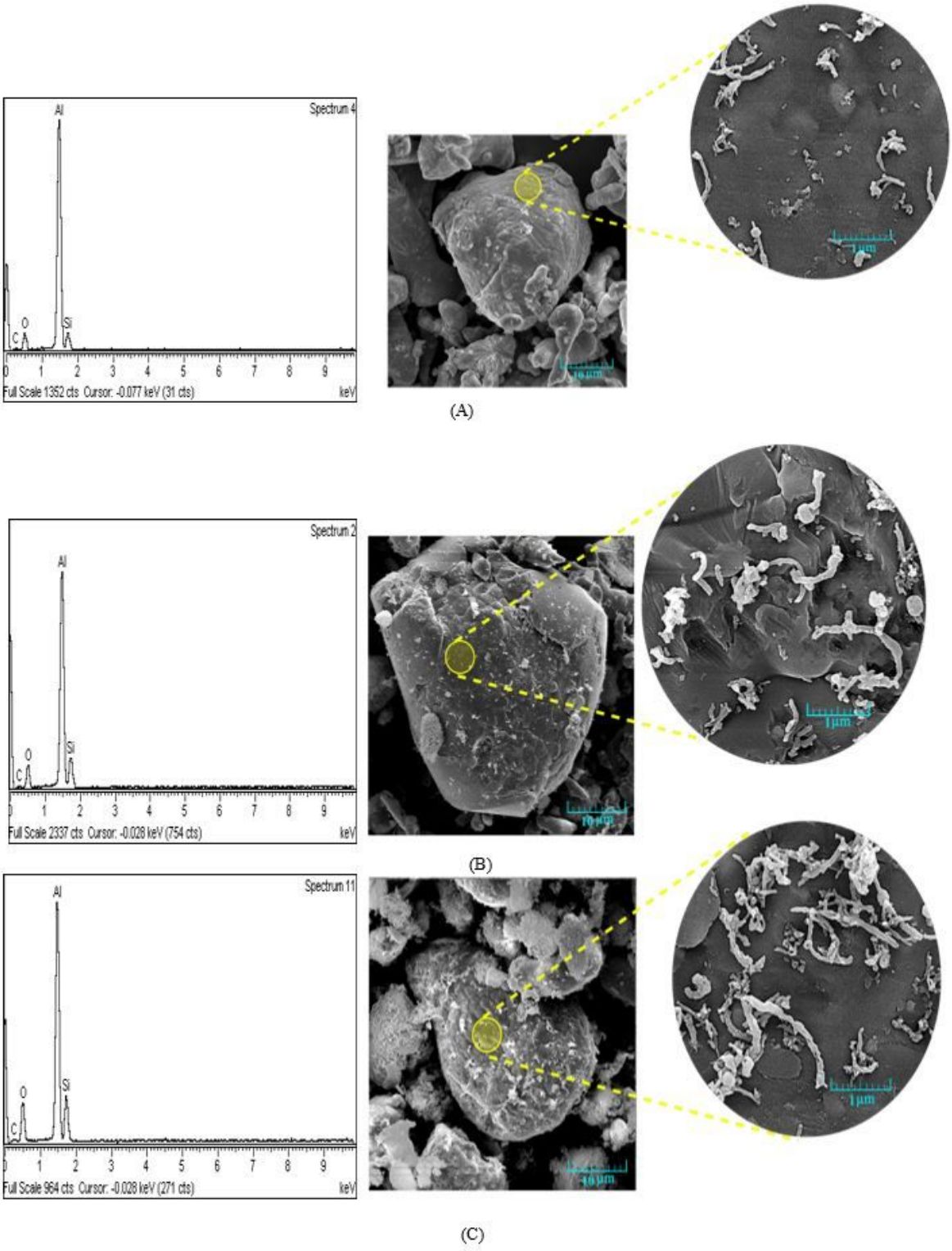

Figure 7

Distribution of a) 3, b) 5 and c) 10 wt % SNTs on Al powders

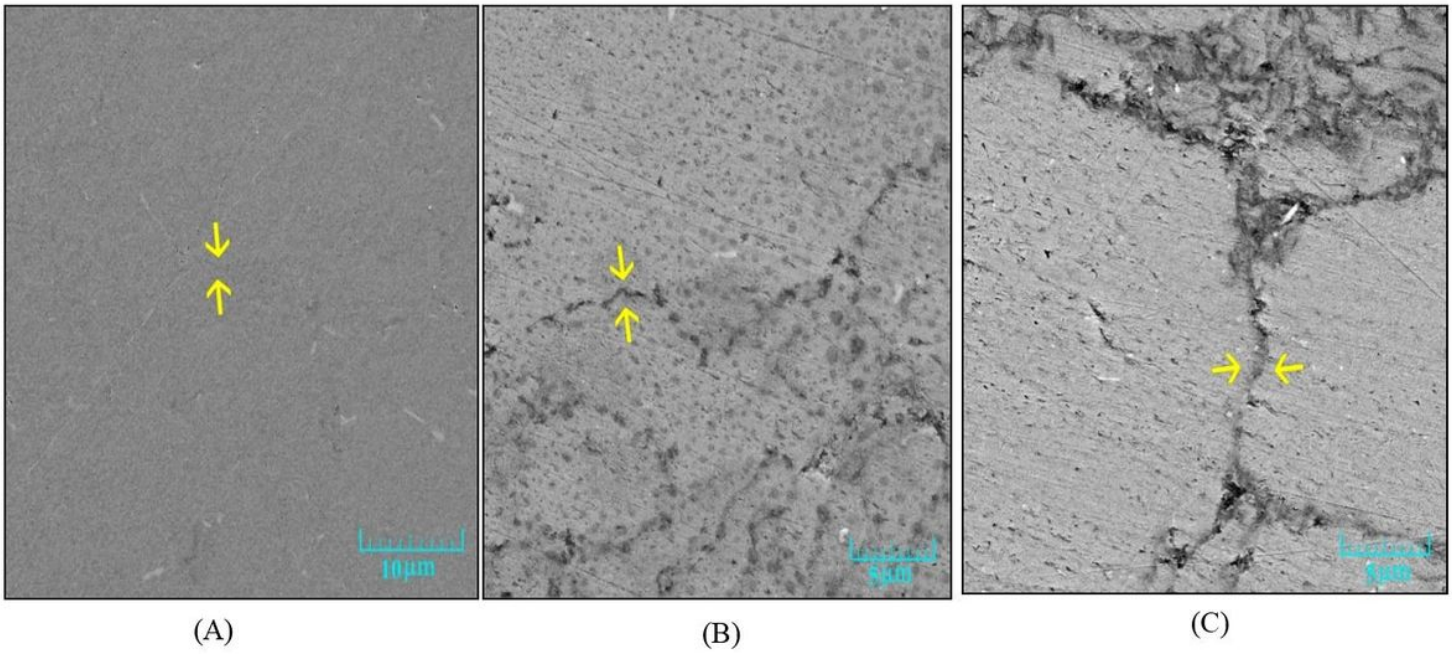

Figure 8

FESEM images of polished surface of composites a) pure Al, b) 3 wt % and c) 5 wt % SiO2 nanoparticles

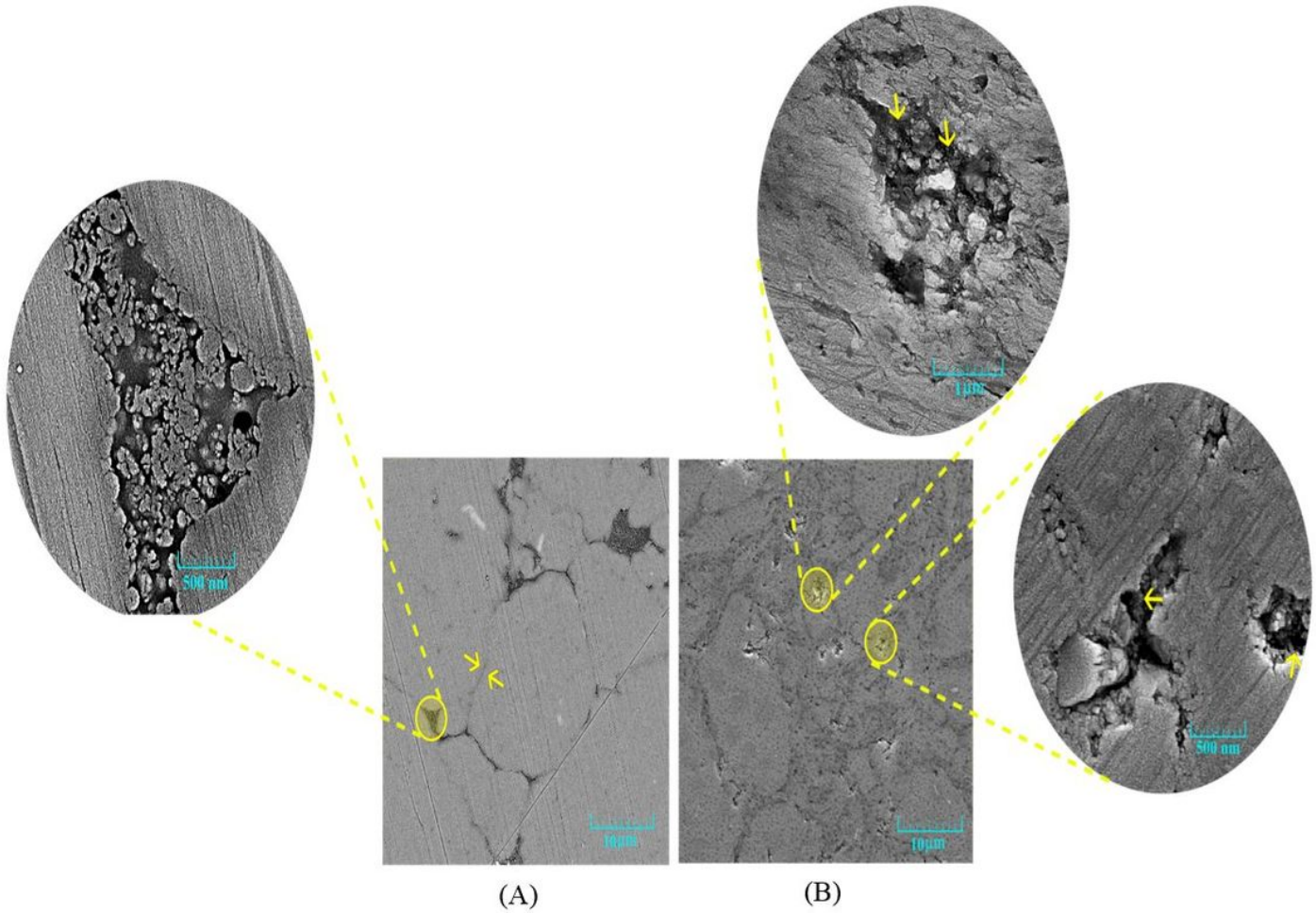

Figure 9

The FESEM images of the composite containing 10 wt % a) SNTs, b) SiO2 nanoparticles after sintering

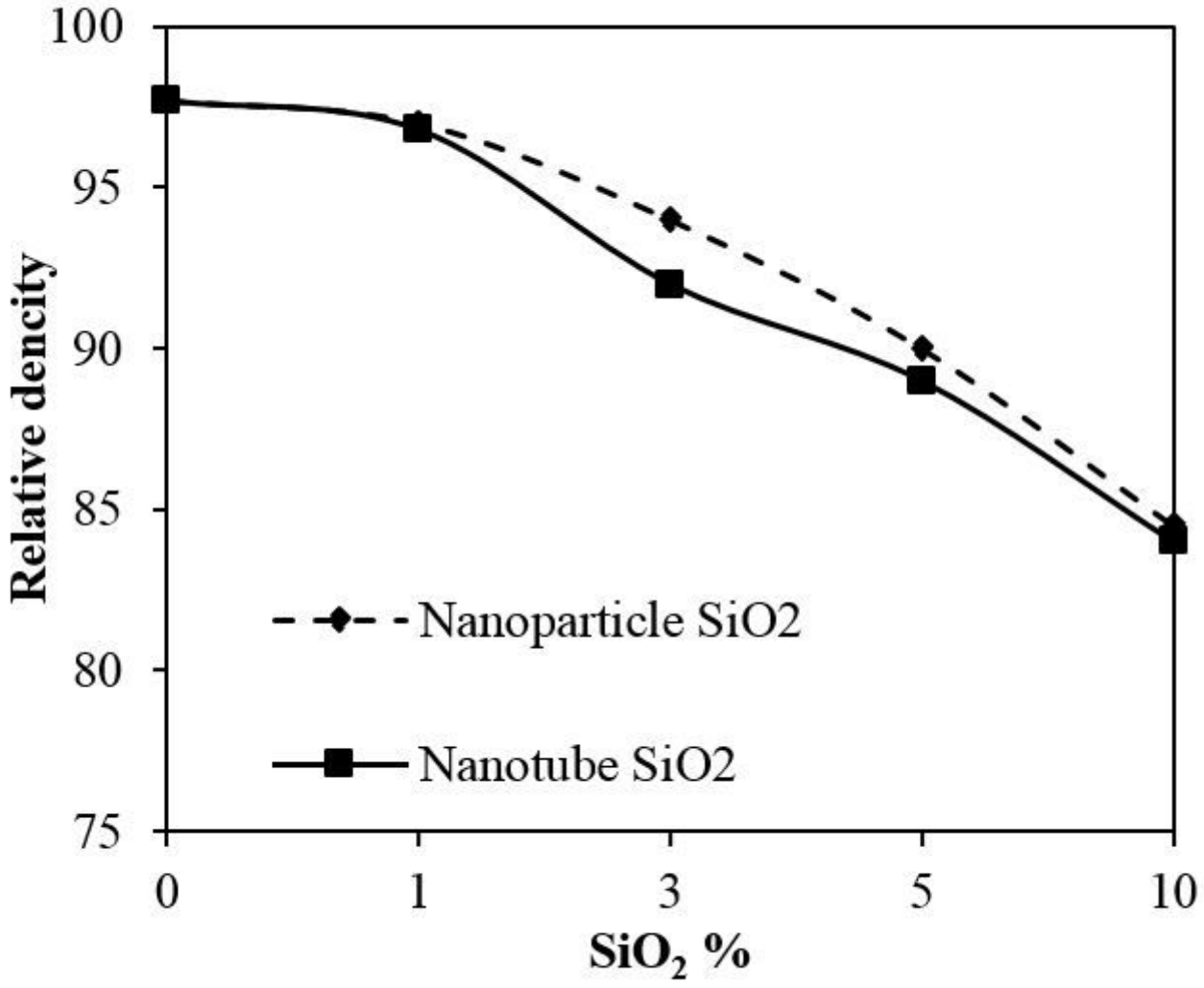

Figure 10

Relative density of the composite as a function of SiO2 weight percent

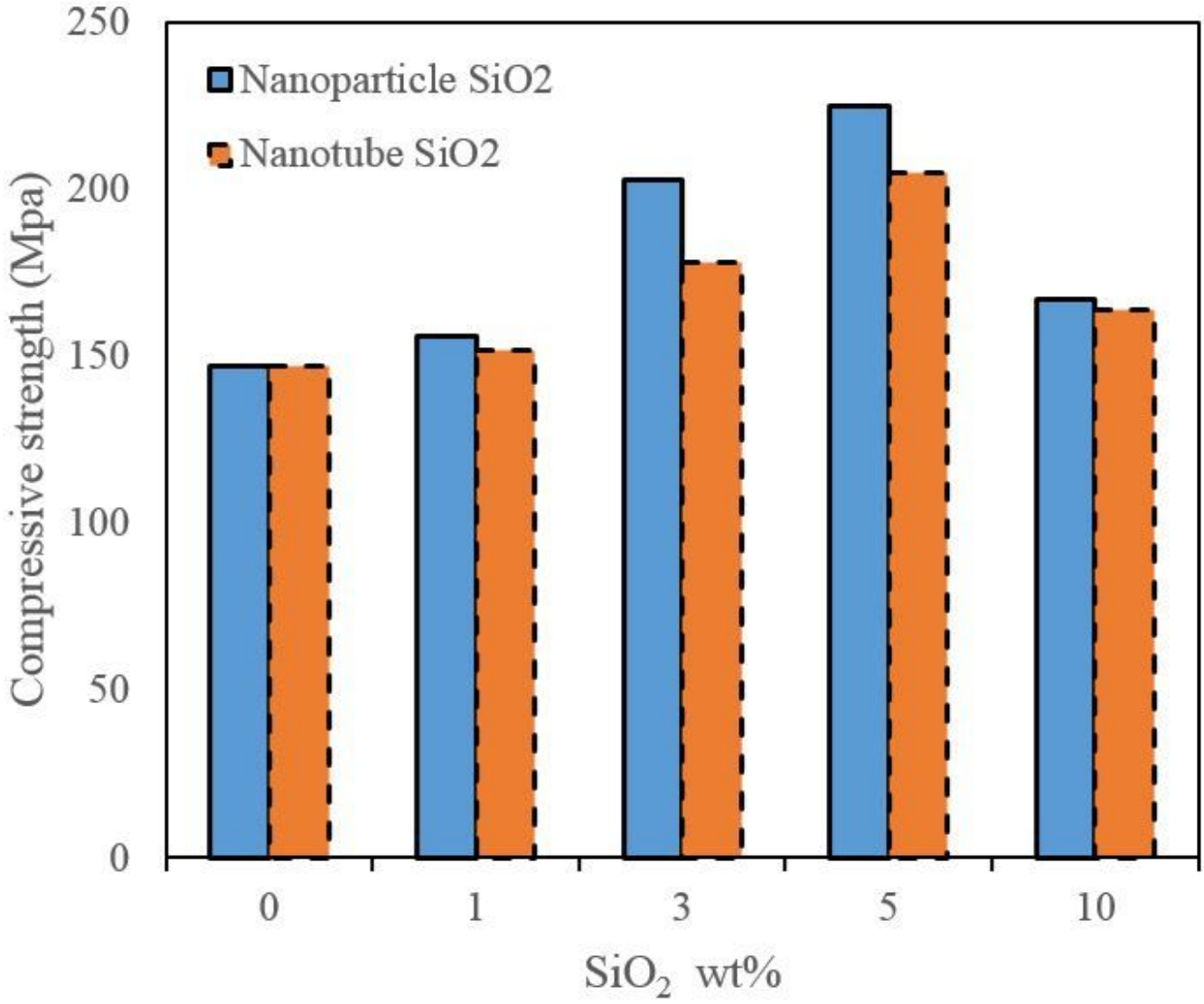

Figure 11

Compressive strength of the composite as a function of SiO2 weight percent.

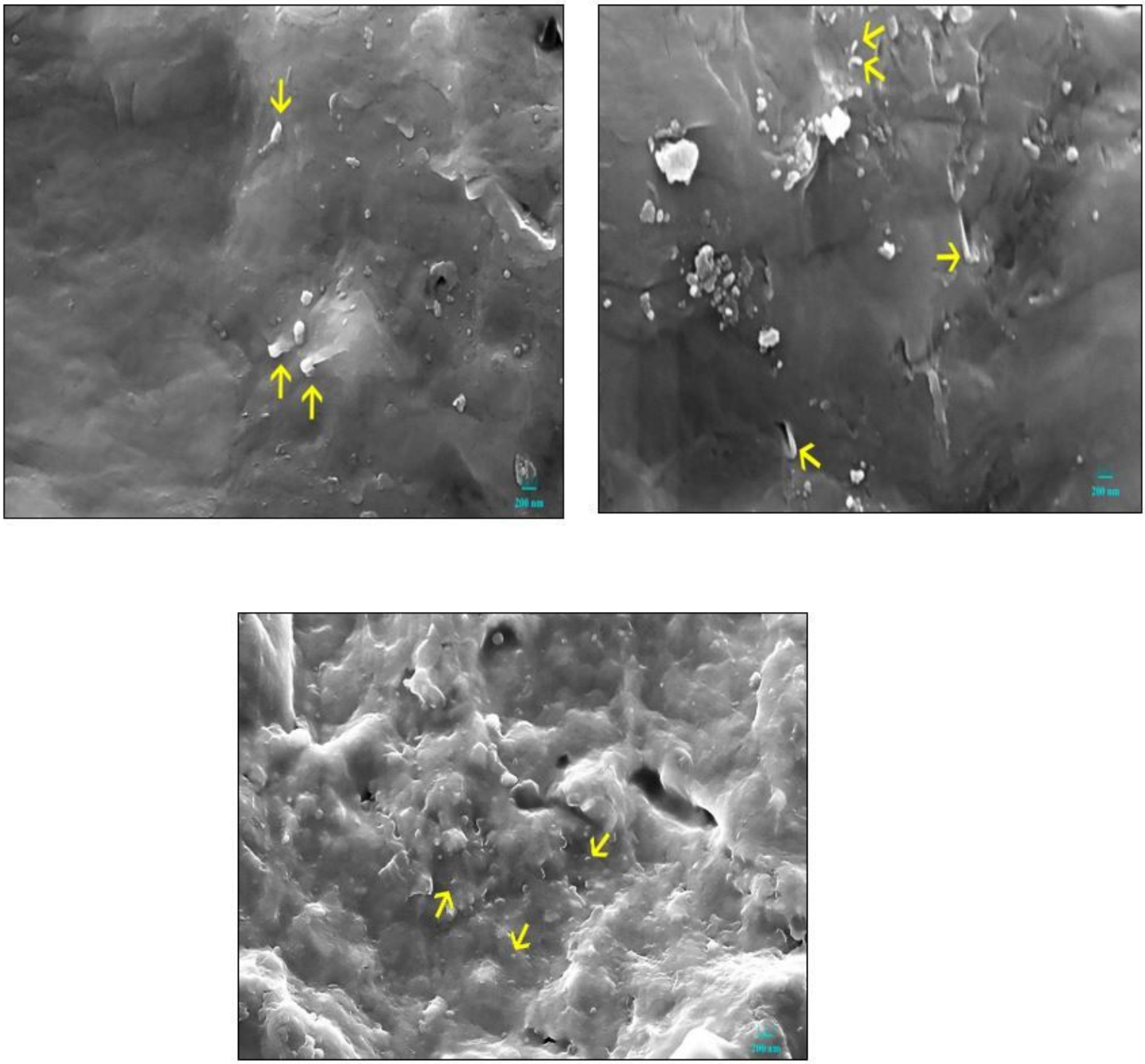

Figure 13

Fracture surface of the composite containing 5 wt % a) SNTs, b) SiO2 nanoparticles

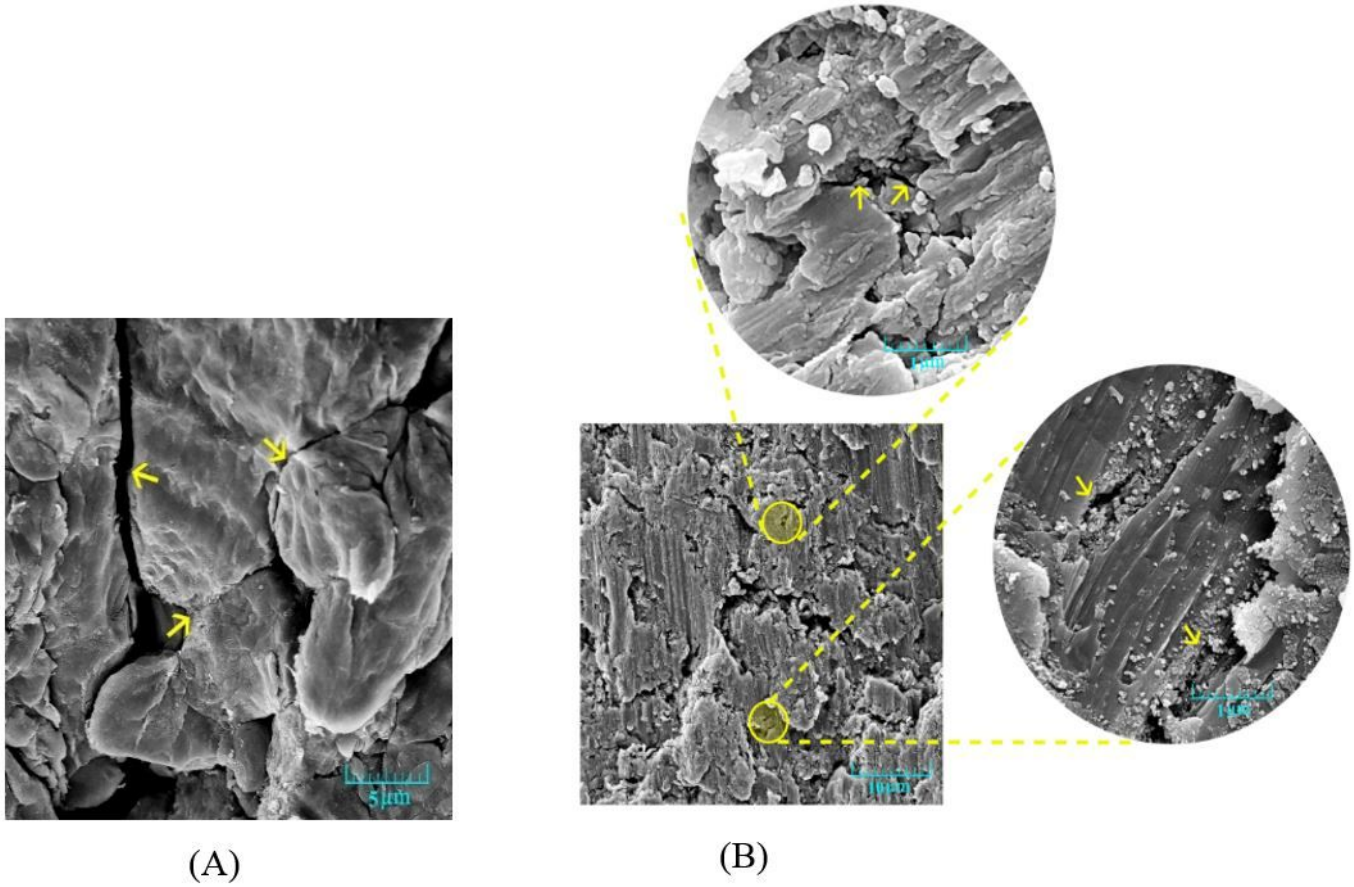

Figure 14

Fracture surface of the composite containing 10% SiO2 nanoparticles

Supplementary Files

This is a list of supplementary files associated with this preprint. Click to download.

- graphicalabstract.docx